RSC Advances

ROYAL SOCIETY OF CHEMISTRY

www.rsc.org/advances

RSC Advances

ARTICLE

A Novel Efficient Mesoporous Silica Assisted Green Emitting Phosphors -An Exotic Remote Phosphor with High Quantum Yield

Received 00th January 20xx,
Accepted 00th January 20xx

DOI: 10.1039/x0xx00000x

www.rsc.org/

Sakthivel Gandhi,[a,c] Kavitha Sakthivel,[b] Bong-Joon Kwon,[a] Hyun-Joo Woo,[a] Ho Sueb Lee,[a] Dong Soo Shin[b] and Kiwan Jang[a,*]

A novel attempt towards the development of Eu^{2+} doped barium silicate and strontium barium silicate has been putforth using a versatile material namely, mesoporous silica through a convenient wet-solid phase reaction. The developed phosphor can be efficiently excited in a broad spectral range of 200 – 500 nm, and gets emitted strongly in the green region. On introduction of strontium to Eu^{2+} doped barium silicate phosphor, a clear red shift has been recorded in the photoluminescence spectra. These mesoporous silica assisted synthesis of $Ba_{1.95}Eu_{0.05}SiO_4$ and $Ba_{0.975}Sr_{0.975}Eu_{0.05}SiO_4$ phosphors showed a good thermal luminescence stability and high quantum efficiency of about 85 %. It has been successfully used for the fabrication of a flexible and translucent remote phosphor. The fabricated remote phosphor attached proto-type LED exhibits a very strong green emission and this can be utilized as an efficient green component for various applications apart from the white LED productions.

Introduction

Nowadays there arises an increased consciousness towards the energy crisis and this makes every individual to search for alternative energy sources for the reduced consumption of power. The invention of blue LED in the last century has opened up new avenues for the transformation of this world towards the illumination source of low energy but with a high-efficiency.[1-4] But, the luminescence suffers from a limiting factor of resultant white light as it is the color of natural sunlight that helps for the maintenance of circadian rhythm of human being.[5] Several strategies had been adopted with careful analysis for the production of white light that includes the use of tri-color LEDs without phosphor and tri, di or mono phosphor along with single LED.[2,4,6&7] Nowadays, the phosphor converted white LEDs is an important area that demands further research effort due to its highly efficient white light emission in addition to its high color rendering index (CRI) and low color correlated temperature (CCT).[8-11] There is also an absence of differential ageing of colors, one of the major obstacles of combined tri-colored white emitting LED devices.[2]

A widely explored material for phosphor application is the divalent europium replaced silicate host crystals owing to its high chemical-thermal stabilities, simple preparative methods and the cost-effectiveness.[12-15] In this contribution, we report on a simple wet-solid phase synthesis of divalent europium introduced barium silicate and barium strontium silicate phosphors. Several reports are available in literature on the preparation of silicate phosphors using a variety of silicate source and by adopting various strategies.[16-21] Most of the research utilizes the conventional silica or the organic tetra ethyl orthosilicate (TEOS) as silicate sources. But, here as a novel input, we have made use of the versatile mesoporous silica (MPS) as the silicate source for the making of phosphor. The results indicate an improvised efficiency along with an excellent quantum yield, when compared to the phosphors prepared using conventional silicate sources.

However, the direct coating of phosphors on LEDs blemishes itself with several difficulties in which the major one is the generation of high temperature.[22] To avoid the misfortunes, here the phosphor has been made as a flexible film and utilized as a remote phosphor. The demand that becomes inevitably pressing in the case of these remote-phosphor converted white LEDs is the high quantum yield. The versatility of mesoporous silica in terms of the high surface area, ordered porosity[8,23-27] and high adsorptivity of cations, make an efficient crystal lattice along with divalent europium dopant which paves the way for a high quantum yield.

Our previous reports rely on the same platform, where a rod like SBA-15 type mesoporous was synthesized and it had been used as silicate source for making $SrCaEuSiO_4$ phosphor for the first time.[8] Its potentiality has been proven in the making of warm white light under blue LEDs with low CCT and high CRI. In the similar lines, various kinds of spherical MPS

[a] Department of Physics, Changwon National University, Changwon, Republic of Korea, Fax: +82-55-213-0263; Tel: +82-055-213-3427.
(*corresponding author E-mail: kwjang@changwon.ac.kr)
[b] Department of Chemistry, Changwon National University, Changwon, Republic of Korea.
[c] Centre for Nanotechnology & Advanced Biomaterials, SASTRA University, Thanjavur, India.

have also been prepared and utilized successfully for the development of same kind of phosphor.[28] Apart from the production of warm white light, the morphology could also be architectured in accordance to the MPS involved. To the best of our knowledge this work is the first of its kind and has not yet been reported so far. In this study we quantify this notion; we investigated the efficacy of the prepared MPS assisted remote phosphor and elucidated its high quantum efficiency & thermal quenching property.

Results and discussion

Figure 1 shows the characterization of the as-synthesized mesoporous silica. The SEM and TEM images given in the Figure 1A & B represent the general external-internal morphologies of MPS and its ordered porous network. The morphology seems to be spherical under high magnification with a diameter of ~400 nm (Inset of Figure 1A). The pores with a diameter of about 2-3 nm can be observed in an ordered hexagonal array (Figure 1B). The nitrogen physisorption study has been done to understand its surface area and exact porous arrangement. The result has been shown in Figure 1C and its inset depicts the BJH isotherm. The results confirm the type IV hysteresis along with the BET surface area of 1200 m^2/g and BJH pore diameter of 3.5 nm. The amorphous nature has been analyzed by the powder XRD that shows a broad diffraction pattern (Figure 1D).

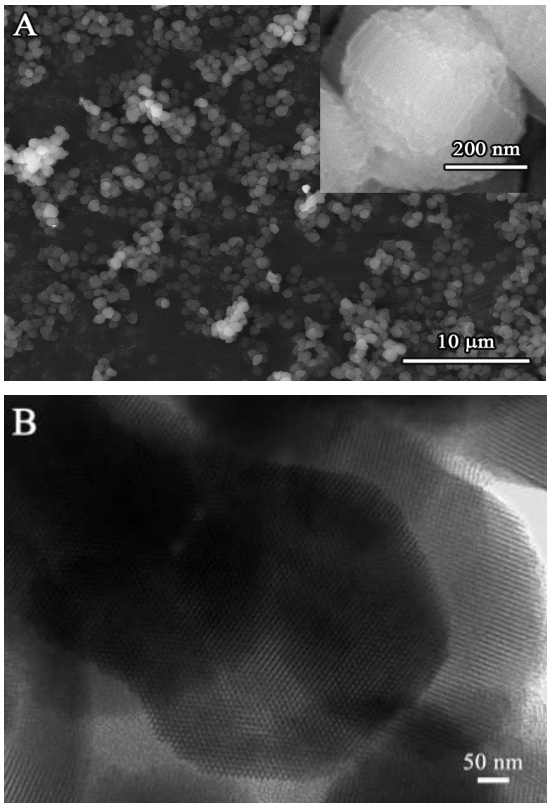

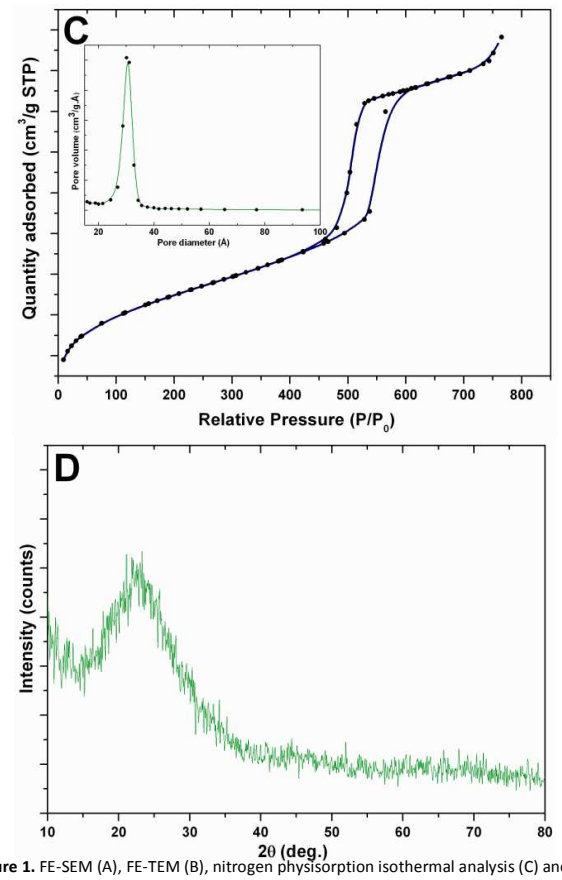

Figure 1. FE-SEM (A), FE-TEM (B), nitrogen physisorption isothermal analysis (C) and powder XRD (D) of MPS. Inset of C depicts the BJH isotherm of MPS.

The XRD patterens of MPS assisted $Ba_{1.95}Eu_{0.05}SiO_4$ and $Ba_{0.975}Sr_{0.975}Eu_{0.05}SiO_4$ phosphors are shown in Figure 2. The XRD pattern of $Ba_{1.95}Eu_{0.05}SiO_4$ phosphor matches well with ICSD database number 36041. This structural confirmation depicts the iso-structural property of this MPS assisted phosphor which means the structural property remains the same with conventional silica assisted $Ba_{1.95}Eu_{0.05}SiO_4$ phosphor but there occurs a difference in the luminescence properties. On introduction of dopant, the crystal structure does not show any second phase, and thus confirming its phase purity. But, there is a small shift in the peaks towards higher degree and this may be ascribed to the shrinkage in the crystal. The reason behind it may be the replacement of bigger Ba^{2+} ion with smaller Eu^{2+} ion. The crystal structure of MPS assisted $Ba_{0.975}Sr_{0.975}Eu_{0.05}SiO_4$ phosphor is shown in Figure 2A&B-c. This has been compared with the prepared $Ba_{1.95}Eu_{0.05}SiO_4$ and reference Ba_2SiO_4 (ICSD No. 36041). A shift in the MPS assisted $Ba_{0.975}Sr_{0.975}Eu_{0.05}SiO_4$ phosphor towards higher 2θ values can be observed when compared with the prepared $Ba_{1.95}Eu_{0.05}SiO_4$ and reference Ba_2SiO_4. This can be attributed to the replacement of smaller Sr^{2+} ion to the bigger Ba^{2+} ionic site of Ba_2SiO_4 host lattice and thus led to the compression of host lattice.

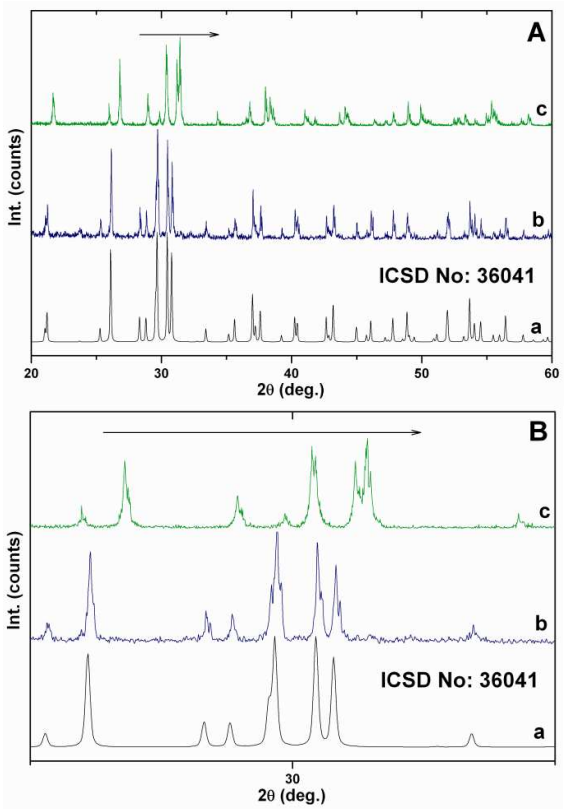

Figure 2. Powder XRD patterns of MPS assisted $Ba_{1.95}Eu_{0.05}SiO_4$ (b) and $Ba_{0.975}Sr_{0.975}Eu_{0.05}SiO_4$ (c) phosphors.

PL excitation and emission spectra of MPS assisted $Ba_{1.95}Eu_{0.05}SiO_4$ & $Ba_{0.975}Sr_{0.975}Eu_{0.05}SiO_4$ phosphors are demonstrated in Figure 3A. The excitation spectra recorded for the emission monitored at 508 nm for $Ba_{1.95}Eu_{0.05}SiO_4$ & 523 nm for $Ba_{0.975}Sr_{0.975}Eu_{0.05}SiO_4$, prove its broad range of absorption from 200 nm to 500 nm. These can be attributed to the transition of electrons from ground state $4f^7$ ($^8S_{7/2}$) to excited $4f^65d^1$ states of Eu^{2+}. In the similar lines, the emission spectra of both the samples excited at 350 nm, show a broad emission between 450 and 650 nm with maximum peak intensities at 508 & 523 nm for $Ba_{1.95}Eu_{0.05}SiO_4$ & $Ba_{0.975}Sr_{0.975}Eu_{0.05}SiO_4$ phosphors, respectively. This is due to the transition of energy from excited $4f^65d^1$ to ground state $4f^7$ of Eu^{2+} ion. The introduction of Sr^{2+} to $Ba_{1.95}Eu_{0.05}SiO_4$ phosphor shows a red shift of ~20 nm with same intensity. These shifts can be well understood with its host crystal structure. Powder XRD also shows a shift in peak towards higher 2θ for MPS assisted $Ba_{0.975}Sr_{0.975}Eu_{0.05}SiO_4$ phosphors due to the compression in the crystal lattice. Moreover, the bond length between Sr^{2+} and Eu^{2+} in $Ba_{0.975}Sr_{0.975}Eu_{0.05}SiO_4$ phosphor is shorter than the bond length of Ba^{2+}-Eu^{2+} in $Ba_{1.95}Eu_{0.05}SiO_4$ phosphor. The shorter bond length reduces the energy due to the increasing crystal field strength and thus shifts the emission to the longer wavelength for Sr^{2+} introduced MPS assisted $Ba_{1.95}Eu_{0.05}SiO_4$ phosphor. The CIE-1931 chromaticity coordinates of MPS assisted $Ba_{1.95}Eu_{0.05}SiO_4$ and $Ba_{0.975}Sr_{0.975}Eu_{0.05}SiO_4$ phosphors upon different excitation wavelengths (350, 400 & 450 nm) are shown in Table 1 and the corresponding color points are noted in the CIE-1931 diagram (Figure 3B). The quantum efficiency of MPS assisted phosphors are also shown in the same table and the values are calculated to be greater than 85%, and more specifically for the phosphors which are efficiently excited at 350 nm.

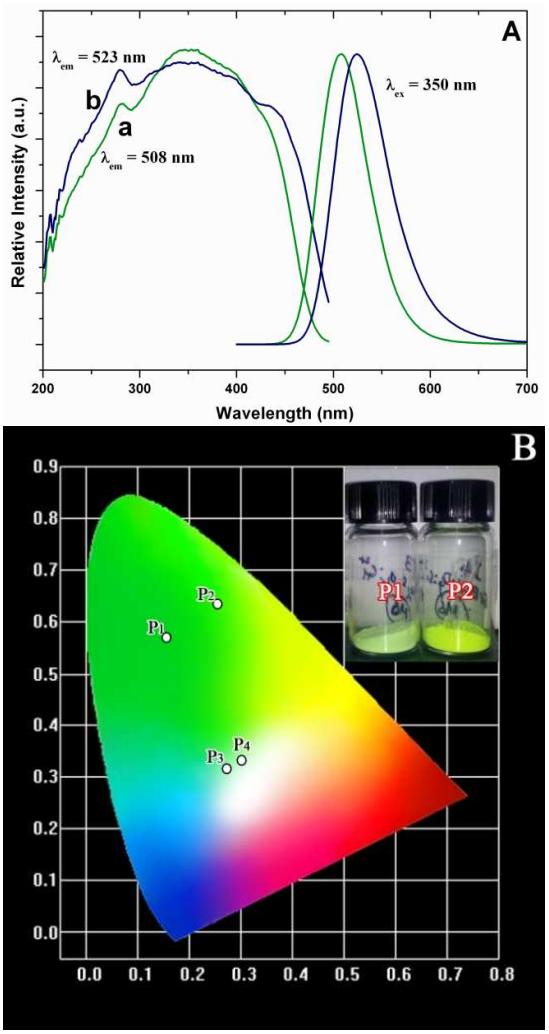

Figure 3. (A) Photoluminescence excitation-emission spectra of MPS assisted $Ba_{1.95}Eu_{0.05}SiO_4$ (a) and $Ba_{0.975}Sr_{0.975}Eu_{0.05}SiO_4$ (b) phosphors. (B) CIE-1931 chromaticity diagram represents the color coordinates of MPS assisted $Ba_{1.95}Eu_{0.05}SiO_4$ (p1), $Ba_{0.975}Sr_{0.975}Eu_{0.05}SiO_4$ (p2) phosphors and proto-type LED fabricated with remote phosphors $Ba_{1.95}Eu_{0.05}SiO_4$ (p3) & $Ba_{0.975}Sr_{0.975}Eu_{0.05}SiO_4$ (p4).

Table 1. CIE chromaticity coordinates and quantum yield of MPS assisted $Ba_{1.95}Eu_{0.05}SiO_4$ and $Ba_{0.975}Sr_{0.975}Eu_{0.05}SiO_4$ phosphors at different excitation wavelengths

Phosphor	Excitation wavelength (nm)	Quantum Yield (%)	CIE1931	
			x	y
$Ba_{1.95}Eu_{0.05}SiO_4$	350	86	0.17(p_1)	0.57(p_1)
	400	65	0.16	0.55
	450	50	0.16	0.57
$Ba_{0.975}Sr_{0.975}Eu_{0.05}SiO_4$	350	89	0.28(p_2)	0.63(p_2)
	400	71	0.27	0.61
	450	58	0.28	0.62

The superior flexibility (g & h) and translucency (a & b) of remote phosphors made using MPS assisted $Ba_{1.95}Eu_{0.05}SiO_4$ (a, c, e & g) and $Ba_{0.975}Sr_{0.975}Eu_{0.05}SiO_4$ (b, d, f & h), are shown in Figure 4A. On the other hand the thickness of both the phosphor films was measured to be ~100 µm. The phosphor films were then assembled on blue emitting LEDs and analyzed for its emission behavior (j & k). The emission from the NUV LED at 3 V was captured and shown in Figure 4A-i. When the remote phosphors are placed on the same NUV LED, the emission color changes to strong green and yellowish green for MPS assisted $Ba_{1.95}Eu_{0.05}SiO_4$ (Figure 4A-j) and $Ba_{0.975}Sr_{0.975}Eu_{0.05}SiO_4$ (Figure 4A-k) phosphors, respectively. Figure 4B shows the electroluminescence spectra of proto-type LEDs made using remote phosphors. The strong blue emission from the LED (Figure 4B-a) excites the remote phosphors of MPS assisted $Ba_{1.95}Eu_{0.05}SiO_4$ (Figure 4B-b) and $Ba_{0.975}Sr_{0.975}Eu_{0.05}SiO_4$ (Figure 4B-c), which emit strong green and yellowish green color, respectively. As there is a difference in the refractive index of silicon resin from LED, the light has been tapped efficiently into the remote phosphor and excites it. Therefore the silicon resin does not show any effect on the emission behavior of remote phosphor. Under the applied voltage of 3 V, a wide and stronger emission band is recorded for both the proto-type LEDs. Consequently, the quantum efficiency of remote phosphors was calculated to be higher than 85%. The color of illuminations from the proto-type LEDs with remote phosphors are confirmed by locating it in the CIE 1931 chromaticity diagram (Figure 3B-p3 & p4).

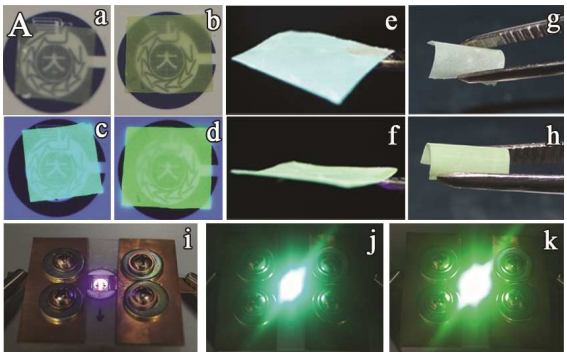

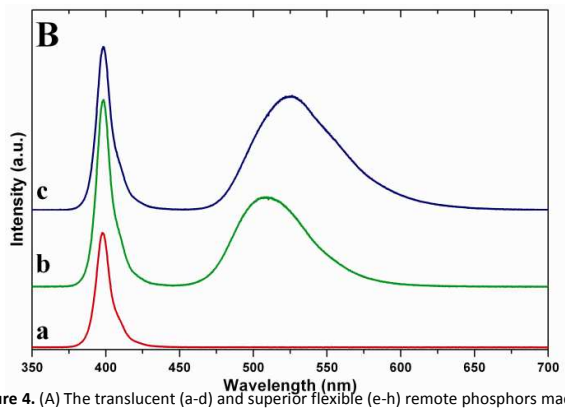

Figure 4. (A) The translucent (a-d) and superior flexible (e-h) remote phosphors made using MPS assisted $Ba_{1.95}Eu_{0.05}SiO_4$ (a, c, e & g) and $Ba_{0.975}Sr_{0.975}Eu_{0.05}SiO_4$ (b, d, f & h). The NUV LED (i) and proto-type LED fabricated with remote phosphors, MPS assisted $Ba_{1.95}Eu_{0.05}SiO_4$ (j) and $Ba_{0.975}Sr_{0.975}Eu_{0.05}SiO_4$ (k). (B) Electroluminescence spectra of NUV LED (a) & proto-type LED fabricated with remote phosphors, MPS assisted $Ba_{1.95}Eu_{0.05}SiO_4$ (b) and $Ba_{0.975}Sr_{0.975}Eu_{0.05}SiO_4$ (c).

Figure 5 shows the thermal stability of MPS assisted $Ba_{1.95}Eu_{0.05}SiO_4$ & $Ba_{0.975}Sr_{0.975}Eu_{0.05}SiO_4$ phosphors and their corresponding films. As the temperature increases gradually from room temperature to 200 °C, the photo emission intensities of all the samples are reduced. On the other hand the emission intensities of remote phosphors are found to subside more smoothly in comparison to the powder samples. The increase in temperature causes the quenching effect which may be ascribed to the photo-oxidation or the damages developed in the crystal. But, the remote phosphor does not undergo for much of the quenching process and this may be attributed to the presence of silicon resin which may protect the phosphor from thermal shock. Although the temperature quenching was recorded as 75% & 49% loss for $Ba_{1.95}Eu_{0.05}SiO_4$ phosphor, a furthermore enhanced result has been attained in the case of $Ba_{0.975}Sr_{0.975}Eu_{0.05}SiO_4$ phosphors which are found to be about only 36% & 16% loss for powders and films, respectively. These pronounced results substantiate the efficacy of these remote phosphors for a wide variety of applications.

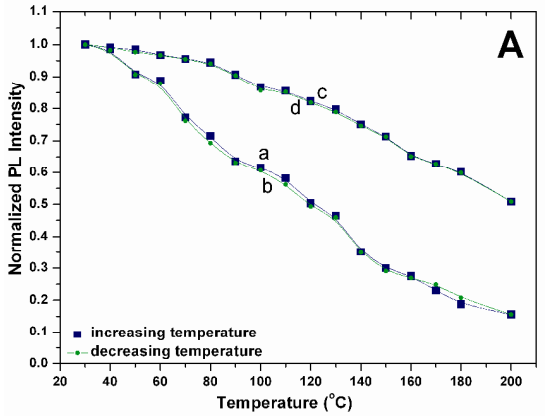

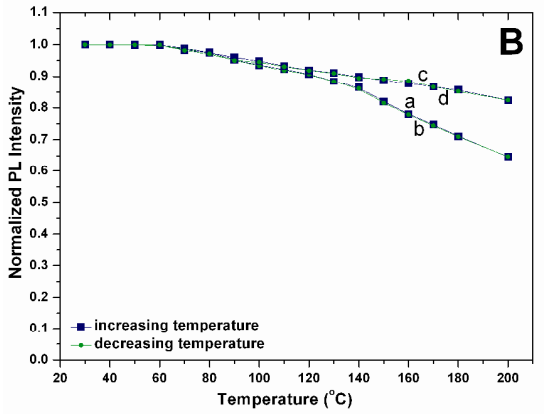

Figure 5. Thermal quenching characteristics of MPS assisted $Ba_{1.95}Eu_{0.05}SiO_4$ (A) and $Ba_{0.975}Sr_{0.975}Eu_{0.05}SiO_4$ (B) phosphor powders (a & b) and remote phosphors (c & d).

Experimental

MPS were prepared in accordance to our earlier report.[21] Briefly, 4 g of P-123 was dissolved in HCl-water-glycerol mixture and the solution was stirred for 4 h. This was followed by the slow addition of silica source and the system was maintained under stirring for another 2 h at ambience. Later, the solution was transferred to a Teflon flask and autoclaved at 80 °C for 24 h to induce the hydrothermal process. The white precipitate obtained was filtered off, washed with deionized water and dried under vacuum at 80 °C. Finally, the dried sample was subjected to 5 h calcination at 550 °C for the removal of organic moieties from the system.

A wet-solid phase strategy was adopted for the preparation of MPS assisted $Ba_2SiO_4:Eu^{2+}$ and $BaSrSiO_4:Eu^{2+}$. Briefly, the above prepared MPS was dispersed in ethanol under sonication process for 2 min duration. It was then followed by the addition of all the cationic sources and subjected to sonication again for 5 more min. The final solution was stirred overnight at the room temperature and at 80 °C for further 12 h. The white dried powder was collected carefully in a crucible followed by heat treatment at 1000 °C for 4 h. The obtained sample was kept at 1200 °C for 2 h under reduced atmosphere (95% N_2/5% H_2) for the reduction of europium ions from its trivalent state to divalency in the host crystal lattice. The optimized concentration of dopant was calculated and the final products have been represented as $Ba_{1.95}Eu_{0.05}SiO_4$ and $Ba_{0.975}Sr_{0.975}Eu_{0.05}SiO_4$, respectively.

The surface morphology of MPS was recorded using field emission scanning electron microscope (FE-SEM, Tescan, MIRA IILMH, Brno, Czech Republic) and the internal porous network was imaged using field emission transmission electron microscope (FE-TEM, JEM 2100F, JEOL, Japan) with an operating voltage of 20 and 200 kV, respectively. Nitrogen physisorption isothermal analysis (Autosorb–1, Quantachrome, USA) was used to understand the surface area and porous arrangements in MPS. The surface area was calculated using BET isotherm whereas BJH isotherm was used to analyze its porous characteristics. Power x-ray diffractometer (XRD, X'Pert Pro, PANalytical) with Ni-filtered Cu-kα1 (λ = 0.154 nm) radiation was used to elucidate the crystalline behavior of prepared MPS assisted $Ba_{1.95}Eu_{0.05}SiO_4$ and $Ba_{0.975}Sr_{0.975}Eu_{0.05}SiO_4$ phosphors.

The photoluminescent excitation and emission of MPS assisted $Ba_{1.95}Eu_{0.05}SiO_4$ and $Ba_{0.975}Sr_{0.975}Eu_{0.05}SiO_4$ phosphors were recorded using a spectrofluorometer (FP–8500, Jasco, Japan) with Xe lamp as an excitation source. The quantum yield was measured using the same instrument which has been equipped with an integrating sphere (ISF-513).

Initially, the phosphor film was made by spin coating technique using silicon resin as a binder. An appropriate ratio of silicon resin & MPS assisted $Ba_{1.95}Eu_{0.05}SiO_4$ or $Ba_{0.975}Sr_{0.975}Eu_{0.05}SiO_4$ phosphors were mixed thoroughly. The prepared phosphor gel was then coated on a Pyrex glass using a spin coater. The parameters namely speed and time were optimized and maintained to be 15 sec and 3000 rpm, respectively. The as-prepared remote phosphors were kept under vacuum for 1 h followed by overnight drying at 80 °C after which the remote phosphor films were peeled off from the glass substrate.

The proto-type LEDs were fabricated by attaching the free-standing flexible and translucent remote phosphors on the near ultra violet (NUV) LEDs (400 nm). The illumination from the LEDs was controlled by a DC power supply (E3633A, Agilent, USA) and the emission behaviors from proto-type LEDs were recorded using an ocean optics luminescence detector (HR4000). Thermal luminescence quenching studies were performed on customized equipment that includes the heater, sensor and an ocean optics luminescence detector (HR4000).

Conclusions

In summary, the current work showed the first time synthesis of an efficient green emitting $Ba_{1.95}Eu_{0.05}SiO_4$ and $Ba_{0.975}Sr_{0.975}Eu_{0.05}SiO_4$ phosphors through a wet-solid phase strategy by the incorporation of the versatile silicate source called mesoporous silica. A translucent and super flexible remote phosphors were made using the MPS assisted $Ba_{1.95}Eu_{0.05}SiO_4$ and $Ba_{0.975}Sr_{0.975}Eu_{0.05}SiO_4$ phosphors. The efficient emission from the fabricated proto-type LEDs along with its high quantum efficiency over 85% and good thermal stability make this phosphor suitable for usage in the various applications that includes the production of warm white light. The designed remote phosphor gives us a bright perspective in the lines of energy consumption and a benign illumination for the maintenance of healthy circadian rhythm.

Acknowledgements

This research was financially supported by Changwon National University (2013–2015).

Notes and references

1 M. S. Shur and A. Zukauskas, *Proc. IEEE,* 2005, **93,** 1691.

2 G. Fasol and S. Nakamura, The Blue Laser Diode: GaN Based Blue Light Emitters and Lasers. Springer, Berlin 1997.
3 E. F. Schubert and J. K. Kim, *Science,* 2005, **308,** 1274.
4 S. Ye, F. Xiao, Y. X. Pan, Y. Y. Ma and Q. Y. Zhang, *Mater. Sci. Eng. R,* 2010, **71,** 1.
5 S. M. Pauley, *Med. Hypotheses,* 2004, **63,** 588.
6 J. S. Kim, P. E. Jeon, J. C. Choi, H. L. Park, S. I. Mho and G. C. Kim, *Appl. Phys. Lett.,* 2004, **84,** 2931.
7 S. Hwang, B. A. Kang, S. Hwangbo, Y. S. Kim and J. T. Kim, *Electron. Mater. Lett.,* 2010, **6**, 27.
8 S. Gandhi, K. Thandavan, B. J. Kwon, H. J. Woo, C. H. Kim, S. S. Yi, J. H. Jeong, D. S. Shin and K. Jang, *J. Mater. Chem. C,* 2014, **2**, 6630.
9 H. Zhu, C. C. Lin, W. Luo, S. Shu, Z. Liu, Y. Liu, J. Kong, E. Ma, Y. Cao, R. S. Liu and X. Chen, *Nat. Commun.,* 2014, **5,** 4312.
10 Y. X. Pan, M. M. Wu and Q. Su, *J. Phys. Chem. Solids,* 2004, **65,** 845.
11 S. Shionoya, W. M. Yen and H. Yamamoto, *Phosphors Handbook*. CRC Press, Boca Raton 1998.
12 M. P. Saradhi and U. V. Varadaraju, *Chem. Mater.,* 2006, **18,** 5267.
13 Y. K. Lee, J. S. Lee, J. Heo, W. B. Im and W. J. Chung, *Opt. Lett.,* 2012, **37,** 3276.
14 Y. Shimomura, T. Honma, M. Shigeiwa, T. Akai, K. Okamoto and N. Kijima, *J. Electrochem. Soc.,* 2007, **154,** J35.
15 Y. H. Song, E. J. Chung, S. H. Song, M. K. Jung, K. Senthil, T. Masaki and D. H. Yoon, *Mater. Lett.,* 2013, **110,** 34.
16 J. K. Park, K. J. Choi, K. N. Kim and C. H. Kim, *Appl. Phys. Lett.,* 2005, **87,** 031108.
17 H. C. Streit, J. Kramer, M. Suta and C. Wickleder, *Materials,* 2013, **6,** 3079.
18 J. I. Choi, M. Anc, A. Piquette, M. E. Hannah, K. C. Mishra, J. B. Talbot and J. McKittrick, *J. Electrochem. Soc.,* 2014, **161,** D111.
19 H. S. Kang, Y. C. Kang, K. Y. Jung and S. B. Park, *Mater. Sci. Eng. B-Adv.,* 2005, **121,** 81.
20 Z. Lu, L. Weng, S. Song, P. Zhang, X. Luo and X. Ren, *Ceram. Int.,* 2012, **38,** 5305.
21 J. K. Han, M. E. Hannah, A. Piquette, J. B. Talbot, K. C. Mishra and J. McKittrick, *J. Lumin.,* 2015, **161,** 20.
22 B. Fan, H. Wu, Y. Zhao, Y. Xian and G. Wang, *IEEE Photon Technol. Lett.,* 2007, **19,** 1121.
23 S. Gandhi, K. Thandavan, B. J. Kwon, H. J. Woo, S. S. Yi, H. S. Lee, J. H. Jeong, K. W. Jang and D. S. Shin, *RSC Adv.,* 2014, **4,** 5953.
24 R. Ravichandran, D. Sundaramurthi, S. Gandhi, S. Sethuraman and U. M. Krishnan, *Micropor. Mesopor. Mat.,* 2014, **187,** 53.
25 S. Gandhi, K. Prem, K. Thandavan, K. W. Jang, D. S. Shin and A. Vinu, *New J. Chem.,* 2014, **38,** 2766.
26 S. Gandhi, S. Venkatesh, U. Sharma, N. R. Jagannathan, S. Sethuraman and U. M. Krishnan, *J. Mater. Chem.,* 2011, **21,** 15698.
27 S. Gandhi, S. Sethuraman and U. M Krishnan, *J. Porous Mat.,* 2014, **21,** 53.
28 S. Gandhi, K. Thandavan, B. J. Kwon, H. J. Woo, D. S. Shin, S. S. Yi, J. H. Jeong and K. W. Jang, *J. Am. Ceram. Soc.,* 2015, DOI: 10.1111/jace.13494.

Graphical Abstract

The MPS assisted remote phosphor attached proto-type LED exhibits a very strong green emission and this can be utilized as an efficient green component for various applications apart from the white LED productions.